Complement C3 and C3aR mediate different aspects of emotional behaviours; relevance to risk for psychiatric disorder

Laura J. Westacott[1,4†], Trevor Humby[1,2†], Niels Haan[1], Sophie A. Brain[2], Emma-Louise Bush[2], Margarita Toneva[7], Andreea-Ingrid Baloc[2], Anna L. Moon[1], Jack Reddaway[1,4], Michael J. Owen[1], Jeremy Hall[1,4], Timothy R. Hughes[3,4], B. Paul Morgan[3,4,6], William P. Gray[1,4,5$] & Lawrence S. Wilkinson[1,2,4*$]

[1] Neuroscience and Mental Health Research Institute, MRC Centre for Neuropsychiatric Genetic and Genomics, School of Medicine, Hadyn Ellis Building, Cardiff University, Cardiff, CF24 4HQ, UK.[2] Behavioural Genetics Group, Schools of Psychology and Medicine, Cardiff University, Cardiff, CF10 3AT, UK. [3] Complement Biology Group, Systems Immunity Research Institute, School of Medicine, Cardiff University, CF14 4XW, Cardiff UK. [4] Hodge Centre for Neuropsychiatric Immunology, School of Medicine, Cardiff University, Cardiff CF24 4HQ, UK. [5] Brain Repair and Intracranial Therapeutics (BRAIN) Unit, School of Medicine, Cardiff University, CF24 4HQ, UK. [6] UK Dementia Research Institute, Cardiff University, Cardiff, CF24 4HQ, UK. [7] Institute of Psychiatry, Psychology and Neuroscience, King's College London, London, SE5 8AF, UK.

[†] These authors contributed equally to the work
[$]Joint senior authors: Lawrence S. Wilkinson & William P. Gray

[*]Corresponding author: Lawrence S. Wilkinson

Email address: WilkinsonL@cardiff.ac.uk

Address: Neuroscience and Mental Health Research Institute, School of Medicine, Cardiff University, Cardiff, CF24 4HQ, UK

Key words: *Complement system, Anxiety, Fear, Stress response.*

Abstract

Complement is a key component of the immune system with roles in inflammation and host-defence. Here we reveal novel functions of complement pathways impacting on emotional reactivity of potential relevance to the emerging links between complement and risk for psychiatric disorder. We used mouse models to assess the effects of manipulating components of the complement system on emotionality. Mice lacking the complement C3a Receptor (*C3aR*$^{-/-}$) demonstrated a selective increase in unconditioned (innate) anxiety whilst mice deficient in the central complement component C3 (*C3*$^{-/-}$) showed a selective increase in conditioned (learned) fear. The dissociable behavioural phenotypes were linked to different signalling mechanisms. Effects on innate anxiety were independent of C3a, the canonical ligand for C3aR, consistent with the existence of an alternative ligand mediating innate anxiety, whereas effects on learned fear were due to loss of iC3b/CR3 signalling. Our findings show that specific elements of the complement system and associated signalling pathways contribute differentially to heightened states of anxiety and fear commonly seen in psychopathology.

1. Introduction

The complement system is a key component of the immune system that plays a pivotal role in inflammation and host-defence. Complement activation occurs via several pathways, all of which lead to cleavage of the central protein, C3 (see Figure S1). Activation of C3 generates the fragments C3a and C3b. C3a is an anaphylatoxin that signals via its canonical G-protein coupled receptor C3aR[1]. Activation of this receptor has been demonstrated to trigger calcium mobilization[2-4], stimulating an array of intracellular signalling pathways to induce both pro- and anti-inflammatory effects[1,5]. C3b on the other hand propagates further complement activation by contributing to the cleavage of complement component 5 (C5) downstream of C3 and, after further cleavage to iC3b, plays a role in opsonisation by macrophages and microglia via complement receptor 3 (CR3). Akin to C3, C5 cleavage generates C5a (another anaphylatoxin and a ligand for the C5a receptor, C5aR) and C5b, which triggers the terminal complement pathway by sequentially binding proteins C6, C7, C8 and C9. These proteins subsequently congregate to assemble the membrane attack complex (MAC) which ultimately results in destruction of the target cell or pathogen via cell lysis[6].

In the central nervous system evidence is emerging that complement has functions beyond its canonical immune roles[7]. Neurons, astrocytes and microglia express complement receptors and regulators, and are also capable of synthesising complement proteins[8,9]. The expression patterns of these vary over the course of brain development[10]. Complement impacts a number of neurodevelopmental processes including neurogenesis[11], migration[12] and synaptic elimination[13] as well as ongoing synaptic plasticity processes underlying learning and memory in the adult brain[14].

95 Furthermore, there is increasing evidence that complement is causally involved in the
96 pathogenesis of neurodegenerative and psychiatric conditions. In Alzheimer's
97 disease, genetic variants in complement related loci have been associated with
98 increased disease risk[15,16], and complement knockout mice exhibit reduced age-
99 related synapse loss[17] and neuropathology[18]. Alterations in complement proteins and
100 activation have also been reported in sera from individuals with autism-spectrum
101 disorder[19] schizophrenia[20], major depressive disorder[21], bipolar disorder[22] and post-
102 traumatic stress disorder[23]. In the case of schizophrenia, an important finding comes
103 from elegant genetic work demonstrating that structural variation in the complement
104 *C4A* locus is associated with risk of developing the disease[24]. C4 cleavage generates
105 fragments that contribute to the activation of C3, yielding C3a and C3b. Given the
106 known roles for the iC3b/CR3 pathway in developmental synaptic pruning[13,25], it has
107 been suggested that *C4A* variants may impact on psychiatric risk via this mechanism,
108 with excessive synaptic elimination leading to abnormal connectivity and disruption of
109 neural networks[24]. Variants in *C3* and putative complement-control genes *CSMD1* and
110 *CSMD2* have also been implicated in genetic susceptibility for schizophrenia[26,27].
111
112 Altered emotional function, in particular maladaptive anxiety and fear, is a pervasive
113 and clinically important symptom in schizophrenia and a frequent comorbidity across
114 several of the DSM-5 and ICD-11 defined disorders. Anxiety and fear exist along a
115 spectrum of aversive emotional states and can be elicited by differing environmental
116 factors to result in distinguishable behavioural outputs[28]. Anxiety is characterised by
117 sustained arousal, hypervigilance and risk assessment surrounding anticipated or
118 potential threats, while fear is often characterised as an acute response to an
119 experienced, imminent danger resulting in immediate avoidance, fight or freezing

behaviour[29,30]. Whilst there is significant overlap in the neurocircuitry underlying these states, there are also contributions from distinct neuronal circuitries[28,31].

There is previous data suggesting complement may play a role in emotional responses to aversive circumstances. Mice overexpressing the human *C4A* variant associated with risk for schizophrenia demonstrated elevated anxiety behaviour[32]. Anxiety phenotypes have also been reported in mice exposed to excessive pre-natal complement activity[33] and neurodegeneration-associated anxiety phenotypes are reduced by complement inhibitors[34]. Furthermore, aged *C3* deficient mice exhibited lower levels of anxiety alongside enhanced learned fear responses[17], whereas increased anxiety has been reported in mice lacking the C3aR[35]. These previous studies suggest that complement can influence both innate and learned aversive behaviours, however, the precise complement signaling pathways responsible for effects on these dissociable aspects of emotionality is unknown.

Utilising the central role of C3 in complement signalling, we used a combination of complement knockout mice to functionally parse innate anxiety and learned fear related phenotypes. In homozygous *C3* knockout mice ($C3^{-/-}$)[36] complement cannot be activated beyond C3, and therefore these animals lack C3 activation fragments (C3a, C3b) and downstream activation products (C5a, C5b) and thus cannot activate the terminal complement pathway. Phenotypes in this model could therefore be the result of loss of any of these downstream effector molecules. We compared the $C3^{-/-}$ model with homozygous *C3aR* knockout mice ($C3aR^{-/-}$)[37]. In these mice, complement is intact apart from the capacity for C3a to bind its canonical receptor C3aR and hence through use of both models, we tested the extent to which phenotypic effects were the

145 result specifically of disrupted C3a/C3aR signalling. A priori, because C3a is an
146 obligate cleavage fragment of C3, we hypothesised that any phenotypes dependent
147 on interaction of C3a and C3aR would be apparent in both *C3*$^{-/-}$ and *C3aR*$^{-/-}$ models.
148
149 Contrary to our initial hypotheses we found clear phenotypic dissociations between
150 the *C3*$^{-/-}$ and *C3aR*$^{-/-}$ models dependent on the nature of the emotional behaviour.
151 *C3aR*$^{-/-}$ mice displayed a profound innate anxiety phenotype that was lacking in the
152 *C3*$^{-/-}$ model. In contrast, when we examined learned fear, where a previously neutral
153 cue generates a fear response as a result of predicting an aversive outcome, we found
154 that the dissociation was reversed with the *C3*$^{-/-}$ mice exhibiting an enhanced fear
155 response to a conditioned cue, but no differences between wildtype and *C3aR*$^{-/-}$mice.
156 This double dissociation in emotionality was linked to distinct underlying complement
157 signalling mechanisms, with anxiety phenotypes in C3aR mice likely to be independent
158 of C3a/C3aR signalling raising the possibility of an alternative ligand for C3aR, and
159 *C3*$^{-/-}$ effects on learned fear likely the result of alterations in iC3b-CR3 pathway activity.
160 These findings point to a hitherto unrecognized complexity of complement effects on
161 brain function and behaviour of relevance to emotional dysfunction in
162 psychopathology.
163

164 ## 2. Materials and Methods

165 **2.1 Mouse models and husbandry.** Wildtype and *C3*$^{-/-}$ strains were sourced in-house
166 from Professor B. Paul Morgan and Dr Timothy Hughes (strains originally from The
167 Jackson Laboratory; B6.PL-Thy1^{a}/CyJ stock#000406 and B6;129S4-C3tm1Crr/J
168 stock#003641 respectively); *C3aR*$^{-/-}$ mice were provided by Professor Craig Gerard of
169 Boston Children's Hospital, USA (strain subsequently provided to The Jackson

170 Laboratory; B6.129S4(C)- *C3ar1*^{tm1Cge}/BalouJ; stock#033904). *C5*$^{-/-}$ mice (as
171 described in [38]) were provided by Professor Marina Botto, Imperial College London.
172 This strain originated from naturally C5-deficient DBA/2J mice, that had been
173 backcrossed to C57Bl/6J. *C3*$^{-/-}$, *C3aR*$^{-/-}$ and *C5*$^{-/-}$ strains were maintained via
174 homozygous x homozygous breeding and were on a C57Bl/6J background. In all
175 experiments, knockout mice were compared to wildtype mice also on a C57Bl/6J
176 background. Mice were between 3-8 months old during experimental testing and were
177 kept in a temperature and humidity-controlled vivarium (21±2°C and 50±10%,
178 respectively) with a 12-hour light-dark cycle (lights on at 07:00hrs/lights off at
179 19:00hrs). Home cages were environmentally enriched with cardboard tubes, soft
180 wood blocks and nesting materials and animals were housed in single sex littermate
181 groups (2-5 mice/cage). Standard laboratory chow and water were available *ad*
182 *libitum*. All procedures were performed in accordance with the requirements of the UK
183 Animals (Scientific Procedures) Act (1986).
184
185 **2.2 General behavioural methods.** Testing took place between the hours of 09:00
186 and 17:00, with random distribution of testing for subjects of different genotypes
187 throughout the day. Mice were habituated to the test rooms for 30 min prior to testing.
188 All assays involved individual testing of mice and apparatus was cleaned thoroughly
189 with a 70% ethanol solution between subjects.
190
191 **2.3 Data collection.** Data for the EPM, EZM and Open Field were collected using
192 EthoVision XT software (Noldus Information Technology, Netherlands) via a video
193 camera mounted above the centre of each piece of apparatus. Tracking of each

194 subject was determined as the location of the greater body-proportion (12 frames/s) in
195 the specific virtual zones of each piece of apparatus.
196
197 **2.4 The elevated plus maze (EPM).** The maze, positioned 300 mm above the floor
198 and illuminated evenly at 15 lux, was constructed of opaque white Perspex and
199 consisted of two exposed open arms (175 x 78 mm^2, length x width, no ledges) and
200 two equally sized enclosed arms, which had 150 mm high walls[39]. Equivalent arms
201 were arranged opposite one another. Subjects were placed at the enclosed end of a
202 closed arm and allowed to freely explore for 5 minutes. Data from each pair of arms
203 were combined to generate single open and closed arm values (number and duration
204 of arm entries and latency of first entry to each arm). In addition, the following
205 parameters were manually scored (by an experimenter positioned at a computer in the
206 same room as the maze, watching the live-video stream of the test); number of stretch-
207 attend postures (SAPs; defined as the animal slowly and carefully reaching towards
208 the open arms in a low, elongated body posture[40,41]) and number of head dips from
209 the open arms (looking down over the edge of an open arm).
210
211 **2.5 The elevated zero maze (EZM).** The maze, positioned 520 mm above the floor
212 and illuminated evenly at 15 lux, was constructed of wood and consisted of two
213 exposed open regions (without ledges; 52 mm wide) and two equally sized enclosed
214 regions (also 52 mm wide), which had 200 mm high grey opaque walls. The diameter
215 of the maze was 600mm. Equivalent regions were arranged opposite one another.
216 Subjects were placed at the border of one of the open and closed regions and allowed
217 to freely explore for 5 min. Data from each pair of regions were combined to generate
218 single open and closed region values (number and duration of region entries and

219 latency of first entry to each region). In addition, the number of head dips (as above)
220 were measured. Due to the high walls of the enclosed sections of the maze, subjects
221 were not visible to the experimenter when in the closed regions and therefore these
222 parameters were scored only when a subject was on the open regions.
223
224 **2.6 Locomotor activity (LMA).** LMA was measured in an apparatus consisting of
225 twelve transparent Perspex chambers (each 210 x 360 x 200 mm, width x length x
226 height). Two infrared beams were embedded within the walls of each chamber, which
227 crossed the chamber 30 mm from each end and 10 mm from the chamber floor.
228 Individual subjects were placed in a designated chamber for a 120 min duration on
229 three consecutive days. Beam breaks were recorded as an index of activity, using a
230 computer running custom written BBC Basic V6 programme with additional interfacing
231 by ARACHNID (Cambridge Cognition Ltd, Cambridge, UK). Data were analysed as
232 the total number of beam breaks per session per day.
233
234 **2.7 Fear-potentiated startle (FPS).** FPS was assessed using startle chamber
235 apparatus which consisted of a pair of ventilated and soundproofed SR-LAB startle
236 chambers (San Diego Instruments, CA, USA) each containing a non-restrictive
237 Plexiglas cylinder (35 mm in diameter), mounted on a Perspex plinth, into which a
238 subject was placed. The motor responses of subjects to white noise stimuli (generated
239 from a speaker 120 mm above the cylinder) were recorded via a piezoelectric
240 accelerometer, attached centrally below the Plexiglas cylinder, which converted
241 flexion plinth vibration into electrical signals. The peak startle response, within 200ms
242 from the onset of each startle presentation, in each trial, was normalized for body
243 weight differences using Kleiber's 0.75 mass exponent[42] as per[43]. A computer running

SR-Lab software (Version 94.1.7.48) was used to programme trials and record data. A foot shock grid connected to a shock generator (San Diego Instruments, CA, USA) was inserted into the Plexiglas cylinder before conditioning sessions.

FPS consisted of three separate sessions presented over a two-day period (see Figure 4A). On the first day, mice were given a pre-conditioning session immediately followed by the conditioning session. The pre-conditioning session started with a 5 min acclimatisation phase followed by presentation of 3 no-stimulus trials, and then a block of pulse-alone trials presented at 90, 100 and 110dB (5 of each at 40 ms duration). Trials were randomly distributed throughout the session and presented with a 60 s random interval (range 36 s to 88 s). After the pre-conditioning session was complete, mice were removed from the startle chambers, restraint tubes cleaned, and shock grids were placed into the Plexiglas cylinders prior to commencing the conditioning session. The mice were then returned to the startle chambers and subjected to a session consisting of a 5 min acclimatisation phase followed by 3 CS+shock trials, with 3 no stimulus trials before and after, presented with a 2min random interval (range 1.5 to 3min). The scrambled 0.14 mA, 0.5 s foot shock was delivered in the final 0.5 s of the 30 s visual CS. Following a 24hr delay, subjects were assessed for FPS in the post-conditioning session. This session followed the same format as the pre-conditioning session (5 min acclimatisation phase followed by presentation of 3 no-stimulus trials, and then a block of pulse-alone trials presented at 90, 100 and 110dB, with 5 of each at 40 ms duration) however the final block of trials also included pulse+CS trials at 90, 100 and 110 dB (5 of each), with the startle pulse presented in the final 40 ms of the CS. FPS was determined as the fold change between pulse-alone trials and pulse+CS trials within the post-conditioning session.

269

270 **2.8 Corticosterone measurements.** Testing took place between the hours of 10:00
271 and 14:00 to account for the diurnal pattern of corticosterone release[44]. Mice were
272 allowed to freely explore the EPM for 5 min, after which they were placed in a holding
273 cage for a further 25 min before being culled by cervical dislocation. Control mice were
274 removed from their home cage and immediately culled. There was an equal
275 distribution of subjects of different genotypes, counterbalanced between the two test
276 conditions and throughout the testing period. Trunk blood was collected into heparin
277 tubes (Becton Dickinson, USA) and immediately centrifuged at 4000 rpm for 10 min,
278 and the supernatant removed and frozen at -80°c until further use. A corticosterone
279 ELISA was performed according to manufacturer's instructions (ADI-900-097, Enzo
280 Life Sciences, UK) and analysed using a four-parameter logistic curve plug in
281 (https://www.myassays.com/four-parameter-logistic-curve.assay).

282

283 **2.9 Diazepam study.** Wildtype, *C3*$^{-/-}$ and *C3aR*$^{-/-}$ were used and were randomly
284 assigned to either vehicle or drug conditions within each genotype. A three-day dosing
285 regimen of diazepam (2 mg/kg, i.p., Hameln Pharmaceuticals, UK) or an equivalent
286 volume of vehicle (0.1 M phosphate buffered saline, pH 7.4) was used, based on pilot
287 testing in wildtype mice to establish an effective anxiolytic dose with minimal sedative
288 effects (data not included). Following 2 days of pre-treatment, diazepam or vehicle
289 was administered 30 min prior to testing on the EPM on the 3rd day.

290

291 **2.10 Tissue for gene expression analysis.** Mice were removed from their home cage
292 and immediately culled via cervical dislocation. Brains were removed and the

293 following regions dissected: medial prefrontal cortex (mPFC), ventral hippocampus
294 (vHPC) and cerebellum (see Figure 6A) and frozen at -80° until further use.
295
296 **2.11 Quantitative Polymerase Chain Reaction (qPCR).** Gene expression was
297 analysed using standardised qPCR methods with quantification using the $2^{-\Delta\Delta Ct}$
298 method[45]. Brain tissue from the mPFC, vHPC and the cerebellum was analysed. RNA
299 was extracted using the RNeasy kit (QIAGEN) and was subsequently treated with
300 DNAse to remove genomic DNA (TURBO DNA-free kit, Thermo Fisher Scientific).
301 RNA was then converted to cDNA (RNA to cDNA EcoDry Premix, Random Hexamers,
302 Clontech, Takara). cDNA samples were run in triplicate in 96 well reaction plates using
303 SYBR-Green-based qPCR (SensiFast, HI-ROX, Bioline) according to manufacturer's
304 instructions using a StepOnePlus System (Applied Biosystems, Thermo Fisher
305 Scientific). Genotypes were counterbalanced across plates and genes of interest were
306 run alongside housekeeping genes *Gapdh* and *Hrpt1* for each sample, within the same
307 reaction plate. All samples were run in triplicate and samples differing by >0.3 Cts
308 were excluded. The change in expression of genes of interest, after normalisation to
309 the two house-keeping genes (ΔCt) was transformed to yield $2^{-\Delta\Delta Ct}$ values. Relative
310 changes from wildtype animals were calculated for each gene of interest.
311
312 **2.12 Primers.** Primers were designed to span at least one exon-exon junction and to
313 match the target sequence only in mouse (Primer-Blast, NCBI) and were synthesised
314 commercially (Sigma Aldrich). Primer efficiency was determined separately through a
315 dilution series of cDNA samples from wildtype hippocampus, cerebellum and cortex.
316 Primers with an efficiency between 90-110% were selected.
317

318 **Table 1**. List of primer sequences used.

Gene	Species	Forward	Reverse
Gapdh	Mouse	GAACATCATCCCTGCATCCA	CCAGTGAGCTTCCCGTTCA
Hprt1	Mouse	TTGCTCGAGATGTCATGAAGGA	AATGTAATCCAGCAGGTCAGCAA
Gabra2	Mouse	AAGCCACTGGAGGAAAACATCT	TTAGCCAGCACCAACCTGAC
Crhr1	Mouse	CTTCAACTCTTTCCTGGAGTCCT	TGGCAGAGCGGACCTCA
Nr3c1	Mouse	AAACTCTGCCTGGTGTGCTC	GGTAATTGTGCTGTCCTTCCAC
Cacna1c	Mouse	ATGGTTCTTGTCAGCATGTTGCGG	TGCAAATGTGGAACCGGTAAGTG
Cacna1d	Mouse	AGAGGACCATGCGAACGAG	CCTTCACCAGAAATAGGGAGTCT
Cacna1e	Mouse	CTCATGTCACCACCGCTAGG	TCTGTCTGCACCACCTTTGG

319

320 **2.13 Genotyping** Genotyping was performed on post-mortem tail tip samples. Qiagen
321 DNeasy Blood and Tissue Kits (Qiagen, Manchester, UK) were used to extract
322 genomic DNA (gDNA) as per the manufacturers standard protocol. For *C3*$^{-/-}$ mice, JAX
323 protocol 27746 was used (common; ATCTTGAGTGCACCAAGCC, wildtype;
324 GGTTGCAGCAGTCTATGAAGG, mutant; GCCAGAGGCCACTTGTATAG) and for
325 *C3aR*$^{-/-}$ JAX protocol 27638 was used (common; AGCCATTCTAGGGGCGTATT, wild
326 type reverse; CATGGTTTGGGGTTATTTCG, mutant reverse;
327 TTGATGTGGAATGTGTGCGAG). For both genotypes, a touchdown cycling protocol
328 was used (see JAX protocols for details). Genotyping for *C5*$^{-/-}$ mice was performed as
329 described in [38].

330

331 **2.14 Statistical analysis.** All statistical analyses were carried out using GraphPad
332 Prism 8.4.1 (GraphPad Software, CA, USA). Data was assessed for equality of
333 variances using the Brown-Forsythe test and then appropriate parametric (*t* test, one-
334 way or two-way ANOVA) or non-parametric (Kruskal-Wallis) tests used. *Post hoc*

335 pairwise comparisons were performed using the Tukey or Dunn's tests for parametric
336 or non-parametric analyses, respectively. For all analyses, alpha was set to 0.05 and
337 exact p values were reported unless $p<0.0001$. All p values were multiplicity
338 adjusted[46]. Data are expressed as mean ± standard error of the mean.
339
340 The main between-subjects' factor for all ANOVA analyses was GENOTYPE (WT, *C3*$^{-}$
341 $^{/-}$, *C3aR*$^{-/-}$, or *C5*$^{-/-}$). For the EPM, LMA and FPS experiments, there were within-
342 subject factors of ZONE (open, closed, middle), DAY (1,2,3) and STIMULUS
343 INTENSITY (90, 100, 110 dB) respectively. Analysis of plasma corticosterone by two-
344 way ANOVA included an additional between subject factor of CONDITION (baseline,
345 EPM), and for the diazepam experiment, there was an additional between subject
346 factor of DRUG (diazepam, vehicle). For qPCR analyses, ΔCt values were analysed
347 by one-way ANOVA.
348
349 **3. Results**
350
351 **3.1 Increased innate anxiety in *C3aR*$^{-/-}$ but not *C3* $^{-/-}$ mice**. Using a cohort of male
352 wildtype, *C3*$^{-/-}$ and *C3aR*$^{-/-}$ mice we first assessed emotional reactivity in the elevated
353 plus maze (EPM), a well-established test of innate anxiety in rodents which exploits
354 the conflict between the drive to explore novel environments and the innate aversion
355 towards open, brightly lit spaces[47,48]. Heatmaps indexing overall maze exploration
356 over a 5-minute session demonstrated major differences in open arm exploration
357 between genotypes (Figure 1A; see Supplementary Video 1 for representative
358 examples). Notably, in comparison to wildtype and *C3*$^{-/-}$ mice, *C3aR*$^{-/-}$ mice took
359 significantly longer to first enter the open arms (Figure 1B) and spent less time on the

open arm per entry (Figure S2A), leading to a reduced overall duration spent in the open arms (Figure 1C), findings consistent with increased anxiety. The ethological parameters head dips and stretch attend postures (SAPs) also differed between genotypes (Figure 1D,E), with *C3aR*$^{-/-}$ mice exhibiting decreases in the former and increases in the latter, a pattern of results again consistent with heightened anxiety[49]. We also noted a significantly increased frequency of head dipping in *C3*$^{-/-}$ mice (Figure 1D), suggestive of reduced levels of anxiety relative to both wildtype and *C3aR*$^{-/-}$ mice[50].

These initial data were consistent with an anxiogenic phenotype present in *C3aR*$^{-/-}$ mice but absent in *C3*$^{-/-}$ mice. We confirmed the findings in two further independent tests of anxiety using additional cohorts of animals. First we used the elevated zero maze (EZM, see Methods Section 2.6), another test of anxiety-like behaviour which similarly probes behavioural responses to exposed, illuminated spaces[51]. The data recapitulated the pattern of findings seen in the EPM (Figure 1F-J). Additional data from the open field test, where *C3aR*$^{-/-}$ mice were more likely to avoid the centre of the arena, were also consistent in demonstrating a specific anxiety-like phenotype in *C3aR*$^{-/-}$ but not *C3*$^{-/-}$ mice (Figure S3). Given that several of the measures indexing anxiety were dependent on movement around the apparatus it was important to eliminate potential locomotor confounds. To address this issue, we measured activity independently in a non-anxiety provoking environment and found no differences in locomotor activity between genotypes (Figure S2C), demonstrating that anxiety measures were unlikely to be influenced by movement confounds. Importantly, experiments conducted in female mice demonstrated comparable *C3aR*$^{-/-}$ anxiety phenotypes in both the elevated plus maze and open field (Figure S6&7).

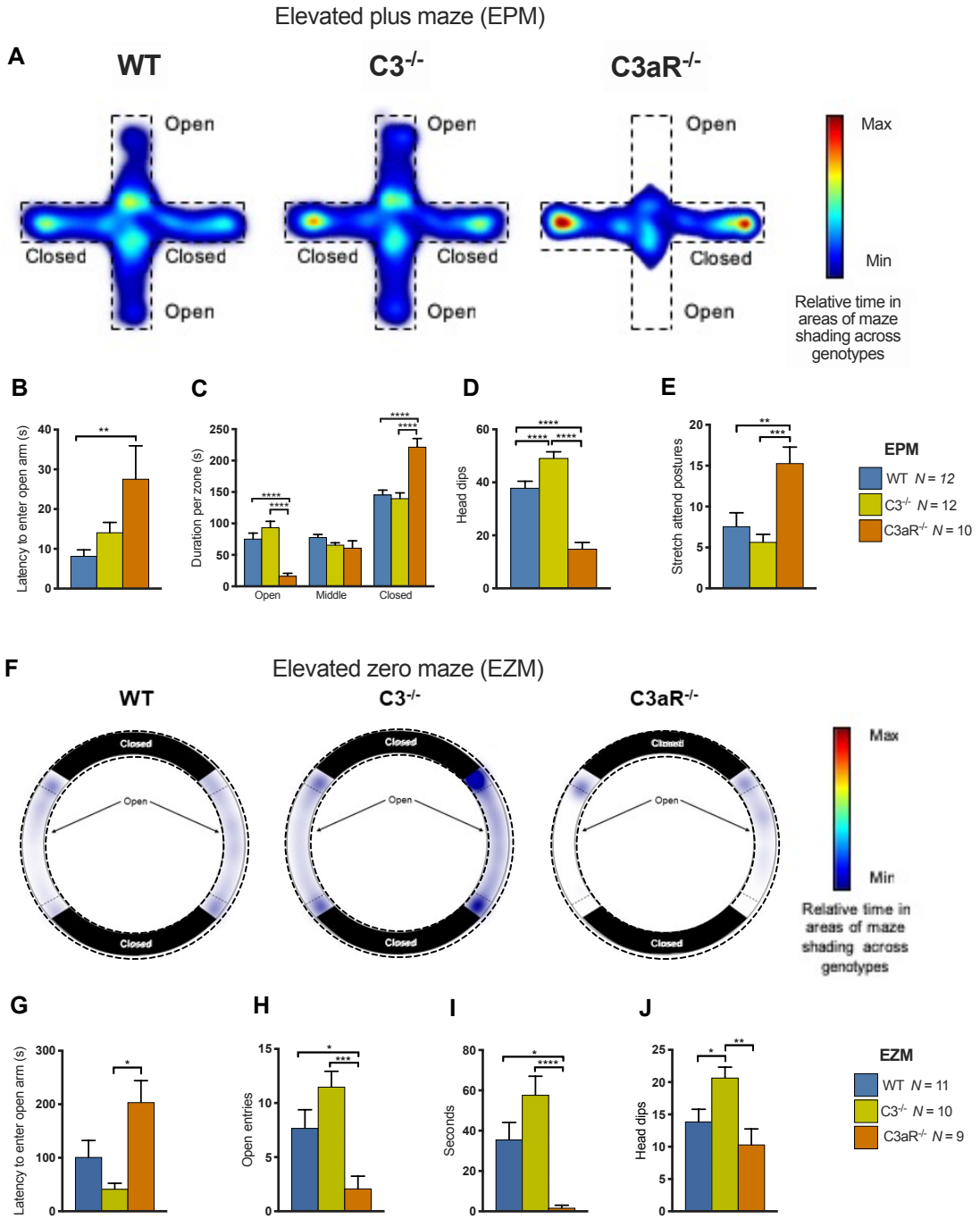

Figure 1. *C3aR*$^{-/-}$, but not *C3*$^{-/-}$ mice show increased anxiety-like behaviour in the elevated plus maze (EPM;A-E) and elevated zero maze (EZM;F-J). (A) Heatmaps displaying relative time per zone of the EPM across genotypes **(B)** Latency to first open arm visit; wildtype 8.21±1.53s, *C3*$^{-/-}$ 14.1±2.52s, *C3aR*$^{-/-}$ 27.6±8.31s, (H_2=10.5, p=0.005). *Post hoc* tests demonstrated that *C3aR*$^{-/-}$ mice took significantly longer to first enter the open arms than wildtype mice (p=0.0045). **(C)** *C3aR*$^{-/-}$ mice distributed

391 their time across the EPM differently to wildtype and *C3*$^{-/-}$ mice (GENOTYPE×ZONE,
392 $F_{4,62}$=17.7, p=0.0001) spending less time in the open arms (*C3aR*$^{-/-}$ 16.70±3.73s vs.
393 wildtype 75.78±8.86s, p<0.0001, *C3aR*$^{-/-}$ vs. *C3*$^{-/-}$ 93.86±9.59s p<0.0001) and
394 significantly more time in the closed arms (*C3aR*$^{-/-}$ 221.88±12.06s vs. wildtype
395 146.01±7.01s, p<0.0001, and *C3*$^{-/-}$ 140.04±8.61s p<0.0001). **(D)** *C3aR*$^{-/-}$ (14.90±2.22)
396 mice performed significantly fewer head dips than wildtype (37.92±2.53, p<0.0001)
397 and *C3*$^{-/-}$ mice (49.17±2.37, p<0.0001), whereas *C3*$^{-/-}$ mice performed significantly
398 more head dips than wildtype mice (p=0.0061; overall ANOVA $F_{2,31}$=48.0, p<0.0001).
399 **(E)** *C3aR*$^{-/-}$ mice performed significantly more stretch attend postures (SAPs;
400 15.30±1.80) than wildtype (7.58±1.66, p=0.0042) and *C3*$^{-/-}$ mice (5.67±0.94, p=0.0004;
401 overall ANOVA $F_{2,31}$=10.3, p=0.0004). **(F)** Heatmaps displaying relative exploration of
402 the open segments of the elevated zero maze, across genotypes. Note that due to the
403 height of the walls in the closed regions it was not possible to track mice or observe
404 ethological behaviours such as grooming or SAPs. **(G)** There was a significant
405 difference in the latency to first enter the open arms (wildtype 101.00±31.00s, *C3*$^{-/-}$
406 42.00±2.52s, *C3aR*$^{-/-}$ 204.00±40.40s, H_2=8.13, p=0.0171). *Post hoc* tests revealed
407 that *C3aR*$^{-/-}$ mice took significantly longer than *C3*$^{-/-}$ mice to initially enter the open
408 region (p=0.0140). **(H)** The number of entries made to open regions differed between
409 genotypes (wildtype 7.69±1.69, *C3*$^{-/-}$ 11.5±1.43s, *C3aR*$^{-/-}$ 2.10±1.15, $F_{2,30}$=8.96,
410 p=0.0009). *C3aR*$^{-/-}$ mice made significantly fewer entries to the open areas than
411 wildtype (p=0.0324) and *C3*$^{-/-}$ mice (p=0.0006) and **(I)** spent significantly less time on
412 the open arms (1.77±1.29) compared to wildtype (35.7±8.43s, p=0.0132) and *C3*$^{-/-}$
413 (57.7±9.32s, p<0.0001; overall Kruskal-Wallis test H_2=19.2, p<0.0001). **(J)** *C3*$^{-/-}$ mice
414 performed significantly more head dips (20.7±1.62) than wildtype (13.9±1.89,

415 p=0.048) and *C3aR*$^{-/-}$ mice (10.3±2.42, p=0.0034; overall ANOVA
416 $F_{2,27}$=6.86,p=0.0039). Data are mean ± S.E.M. *, **, *** and **** represent p≤0.05,
417 p≤0.01, p≤0.001 and p≤0.0001 for *post-hoc* genotype comparisons, respectively.
418

419 **3.2 Neuroendocrine response in *C3aR*$^{-/-}$ and *C3*$^{-/-}$ mice following exposure to the**
420 **elevated plus maze**

421 We next tested whether the behavioural measures of anxiety were paralleled by
422 changes in plasma levels of the stress hormone corticosterone. In a separate cohort
423 of wildtype, *C3*$^{-/-}$ and *C3aR*$^{-/-}$ male mice, we assayed plasma corticosterone 30 minutes
424 after exposure to the EPM and compared levels to those of a group of animals who
425 remained in their home-cages. There were no genotype differences in basal
426 corticosterone levels; however, being placed on the EPM increased plasma
427 corticosterone 6-15-fold in all genotypes, demonstrating that the EPM was a potent
428 stressor (Figure 2A). *Post hoc* analyses showed a significantly greater EPM-evoked
429 corticosterone response in the *C3aR*$^{-/-}$ animals, consistent with their increased
430 anxiety-like behaviour observed on the maze.
431
432

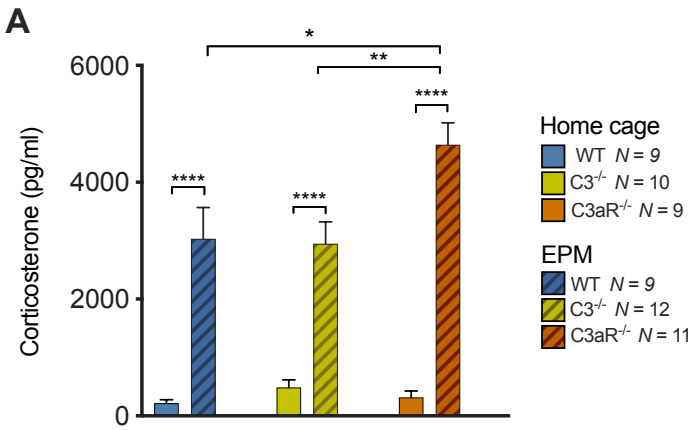

433

434 **Figure 2. Neuroendocrine response following exposure to the elevated plus**
435 **maze (A)** 5-minute exposure to the EPM significantly elevated corticosterone in all
436 genotypes (main effect of CONDITION, $F_{1,54}$=143, p<0.0001; baseline 344.66±63.70
437 vs. EPM 3553.84±274.13). There was a significant GENOTYPE × CONDITION
438 interaction ($F_{2,54}$=4.64, p=0.0138). *Post hoc* analysis showed that after the EPM,
439 *C3aR*$^{-/-}$ mice demonstrated significantly higher corticosterone levels (4640.27±376.13)
440 than wildtype (3033.78±535.06, p=0.0127) and *C3*$^{-/-}$ mice (2948.00±374.87,
441 p=0.0032). *Post hoc* tests also indicated that there were no baseline differences
442 between genotypes (wildtype 216.54±63.2 vs. *C3aR*$^{-/-}$ 316.17±111.60 p>0.9999,
443 wildtype vs. *C3*$^{-/-}$ p=0.9927, and *C3*$^{-/-}$ 485.60±130.35 vs.*C3aR*$^{-/-}$ mice p=0.9992). Data
444 represent mean + S.E.M. *, **, and **** represent p≤0.05, p≤0.01 and p≤0.0001 for
445 *post-hoc* genotype comparisons, respectively.
446
447
448 **3.3 Altered sensitivity of *C3aR*$^{-/-}$ and *C3*$^{-/-}$ mice to diazepam in the elevated plus**
449 **maze**
450 In a further independent cohort of male mice, we tested the sensitivity of EPM induced
451 anxiety-like behaviour to the benzodiazepine diazepam, an established clinically
452 effective anxiolytic drug[47,52]. Our initial behavioural findings were replicated in vehicle-
453 treated animals across all behavioural indices of anxiety, again showing an anxiogenic
454 phenotype in *C3aR*$^{-/-}$ but not *C3*$^{-/-}$ mice (Figure 3A). As anticipated, in wildtype mice
455 2mg/kg diazepam led to a trend for increased time on the open arms (Figure 3B) and
456 a significant reduction in SAPs which are considered to reflect risk assessment
457 behaviour[53-55](Figure 3C). These effects were therefore consistent with reduced
458 anxiety[50,55]. In contrast, the same dose of drug that was effective in eliciting anxiolysis

459 in wildtypes was without effects in *C3aR*$^{-/-}$ mice (Figure 3A,B,C) and produced a
460 seemingly anxiogenic (increased anxiety) pattern of effects in *C3*$^{-/-}$ mice (Figure 3A,B
461 and Figure S4B,C). Locomotor activity monitored across all the maze (Figure S4D)
462 indicated that wildtype and *C3aR*$^{-/-}$ mice were unlikely to have been influenced by
463 diazepam-induced sedation. In *C3*$^{-/-}$ mice however, activity was significantly
464 suppressed under drug conditions indicating a possible sedative effect. Together,
465 these data indicated a fundamentally altered reactivity to diazepam in both *C3*$^{-/-}$ and
466 *C3aR*$^{-/-}$ models.
467
468

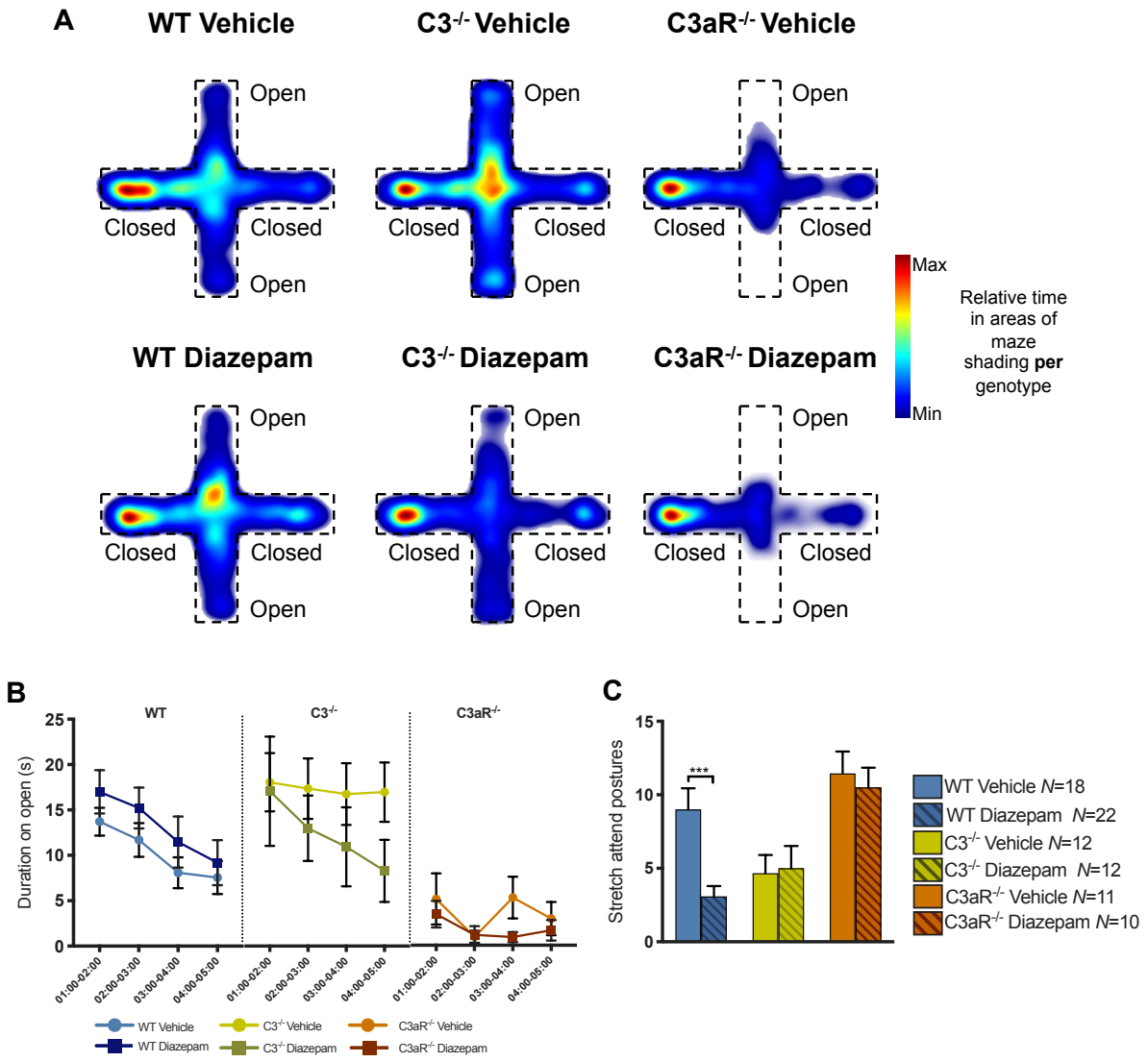

469

470 **Figure 3. Altered sensitivity to diazepam in *C3aR*$^{-/-}$ and *C3*$^{-/-}$ mice.** Behaviourally
471 naïve mice were treated with either diazepam (2mg/kg, i.p) or vehicle injections once
472 daily for 2 days and then 30 minutes prior to testing. (**A)** Heatmaps demonstrating
473 duration spent in zones of the maze by vehicle treated and diazepam treated animals
474 **(B)** Plots showing duration spent on open arms in 1-minute time bins (start-01:00 was
475 excluded due to effect of diazepam in delaying initial entry to open arms across
476 genotypes, see Supplementary Figure 4A). There was a trend for wildtype diazepam
477 treated animals to spend more time on the open arms throughout the task although
478 this did not reach significance (main effect of DRUG, $F_{1,38}$=1.41, p=0.2462). In *C3*$^{-/-}$
479 mice there was a strong tendency for drug treated animals to explore the open arms
480 less than vehicle treated *C3*$^{-/-}$ mice (main effect of DRUG, $F_{1,22}$=1.25, p=0.2764). A
481 similar, though less pronounced pattern was seen in *C3aR*$^{-/-}$ mice (main effect of
482 DRUG, $F_{1,19}$=1.55, p=0.2284) **(C)** There were genotype differences in SAPs (main
483 effect of GENOTYPE, $F_{2,79}$=10.7, p<0.0001), a main effect of DRUG ($F_{1,79}$=4.13,
484 p=0.0454) and a significant GENOTYPE × DRUG interaction ($F_{2,79}$=4.64, p=0.0138).
485 *Post hoc* tests showed that diazepam significantly reduced the number of SAPs in
486 wildtype mice only (wildtype vehicle 9.00±1.44 vs. wildtype diazepam 3.09±0.71,
487 p=0.0006, *C3*$^{-/-}$ vehicle 4.67±1.24 vs. *C3*$^{-/-}$ diazepam 5.00±1.51, p=0.9975, *C3aR*$^{-/-}$
488 vehicle 11.45±1.49 vs. *C3aR*$^{-/-}$ diazepam 10.50±1.34, p=0.9558). Data are mean +
489 S.E.M. *, **, and *** represent p≤0.05, p≤0.01 and p≤0.001 for *post-hoc* genotype
490 comparisons, respectively.
491
492
493
494

495 **3.4 Enhanced fear learning in *C3*$^{-/-}$ but not *C3aR*$^{-/-}$ mice**

496 Psychiatric disorders are associated with maladaptive responses to both innate and
497 learned aversive stimuli[56,57]. We therefore extended our analysis to investigate
498 whether the behavioural dissociations in innate anxiety observed between *C3*$^{-/-}$ and
499 *C3aR*$^{-/-}$ mice would also apply to learned or conditioned fear, where a previously
500 neutral cue generates a fear response as a result of predicting an aversive outcome.
501 In a further group of male mice, we used the fear-potentiated startle (FPS)
502 paradigm[30,58] a well-established method of generating learned fear responses to an
503 acute and imminent danger signal that is characteristic of fear. In this paradigm (see
504 Figure 4A and Methods Section 2.7) fear learning is indexed by an enhanced response
505 to a startling noise in the presence of a cue (the conditioned stimulus or CS) previously
506 paired with mild foot shock (the unconditioned stimulus). In the pre-conditioning
507 session, pulse-alone trials revealed increased basal startle reactivity in both *C3aR*$^{-/-}$
508 and *C3*$^{-/-}$ mice relative to wildtype (Figure 4B). Increased reactivity to the unconditioned
509 foot shock stimulus (in the absence of any startle stimulus) during the conditioning
510 session was also observed in both knockouts (Figure 4C). However, these common
511 effects of genotype were not seen in the fear-potentiated startle measures which index
512 fear learning. Whilst all groups showed the expected enhancement of the startle
513 response in the presence of the CS, the effect of the CS was significantly greater in
514 *C3*$^{-/-}$ animals relative to the *C3aR*$^{-/-}$ and wildtype mice (Figure 4D), indicating enhanced
515 learning of the fear related-cue by the *C3*$^{-/-}$ mice. This pattern of effects was also
516 observed in female mice (Figure S8). This was the opposite pattern of effects to those
517 observed in the tests of innate anxiety and showed a double dissociation in the impact
518 of manipulating C3 and C3aR function that depended fundamentally on the nature of
519 the aversive stimulus.

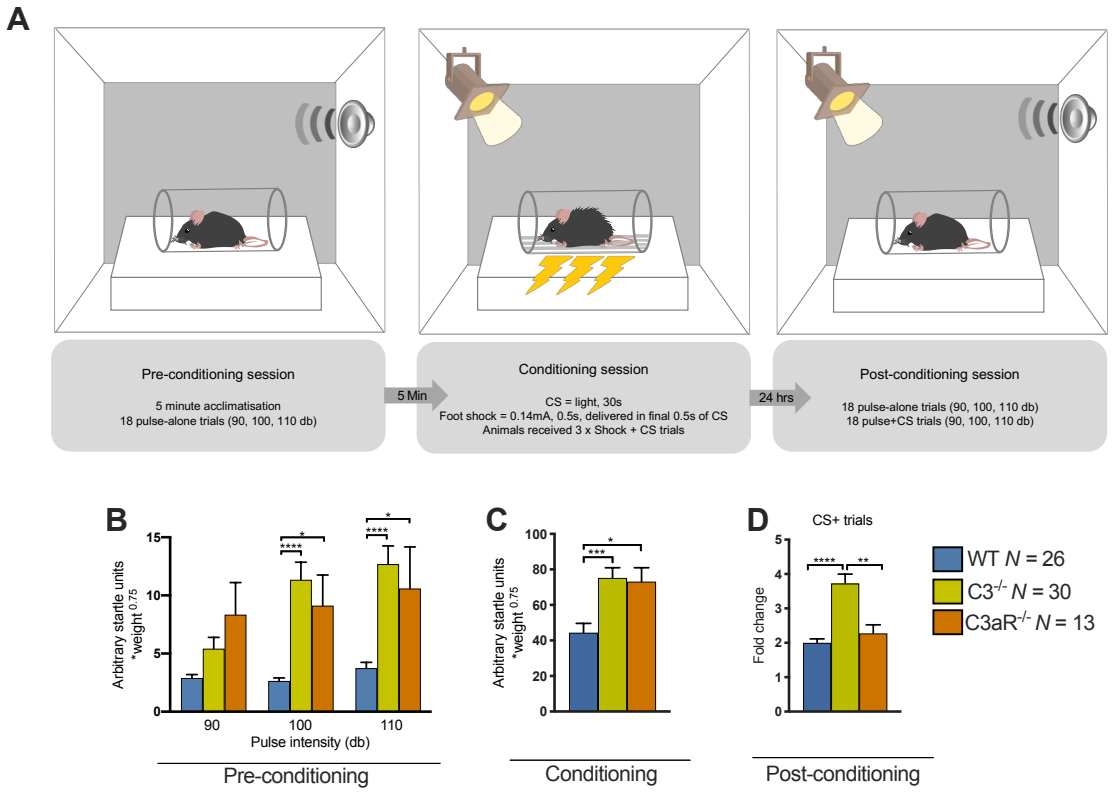

Figure 4. Enhanced fear-potentiated startle in *C3*$^{-/-}$ but not *C3aR*$^{-/-}$ mice. (A) Flow chart depicting the FPS protocol used, which took place in three separate sessions over two consecutive days. Baseline startle reactivity to a range of pulse intensities was assessed in the pre-conditioning session, immediately preceding the conditioning session in which a visual stimulus (light) was paired with 3 weak foot shocks. 24 hours later, subjects were re-introduced to the same chamber and startle reactivity was compared between pulse-alone trials and pulse+CS trials to determine the degree of FPS. On all trials, the peak startle response was recorded and normalised for body weight differences using Kleiber's 0.75 mass exponent, and fold-changes calculated. **(B)** There was a significant main effect of GENOTYPE ($F_{2,66}$=9.04, p=0.0003) and a significant GENOTYPE × STIMULUS INTENSITY interaction ($F_{4,132}$=7.55, p<0.0001). *C3*$^{-/-}$ and *C3aR*$^{-/-}$ mice demonstrated increased levels of startle responding relative to wildtype mice at 100dB (*C3*$^{-/-}$ 11.34±1.51 vs. wildtype 2.63±0.26, p<0.0001, *C3aR*$^{-/-}$

535 9.12±2.63 vs. wildtype p=0.0174) and 110dB (*C3*$^{-/-}$ 12.69±1.55 vs. wildtype 3.74±0.50,
536 p<0.0001, *C3aR*$^{-/-}$ 10.58±3.58 vs. wildtype p=0.0111) **(C)** *C3*$^{-/-}$ and *C3aR*$^{-/-}$ mice also
537 showed increased startle responding to the footshock+CS (*C3*$^{-/-}$ 75.18±5.73, *C3aR*$^{-/-}$
538 73.14±7.78) pairings relative to wildtype mice (44.34±5.29, *C3*$^{-/-}$ vs. wildtype p=0.0006,
539 *C3aR*$^{-/-}$ vs. wildtype p=0.0137, overall ANOVA $F_{2,66}$=8.7, p=0.0004), although it should
540 be noted that responses were much greater to these stimuli in all mice than to the
541 startle stimuli in the pre-conditioning session. **(D)** In the post-conditioning session, all
542 mice demonstrated increases to the pulse+CS stimuli in comparison to pulse-alone
543 stimuli, as demonstrated by the fold-change increase in startle responding, however,
544 this effect was significantly increased in *C3*$^{-/-}$ mice (3.72±0.27) relative to wildtype
545 (1.99±0.11, p<0.0001) and *C3aR*$^{-/-}$ mice (2.27±0.24, p=0.0056, overall Kruskal-Wallis
546 test H_2=27.7, p<0.0001). Data are mean + S.E.M. *, **, *** and **** represent p≤0.05,
547 p≤0.01, p≤0.001 and p≤0.0001 for *post-hoc* genotype comparisons, respectively.

548
549
550

551 **3.5 Complement signalling pathways underlying abnormal learned fear**
552 **phenotypes in *C3*$^{-/-}$ mice**

553 Given the central role of C3 within the complement system, its deletion affects a
554 number of distal pathways (Figure 5A), with the activity of the C3a/C3aR, C3b/CR3,
555 C5a/C5aR and terminal pathways affected. Therefore, the loss of function of any of
556 these pathways may have contributed to the observed fear learning phenotype in *C3*$^{-}$
557 $^{/-}$ mice. However, it is possible to exclude effects due to loss of the C3a/C3aR pathway
558 since the fear learning phenotype was specific to *C3*$^{-/-}$ and not *C3aR*$^{-/-}$ mice (Figure
559 4D). This left iC3b/CR3 signalling and/or pathways downstream of C5 (i.e. C5a/C5aR,
560 terminal pathway) as the remaining possibilities. In order to distinguish between these

561 pathways, we repeated the FPS experiment with the addition of *C5*$^{-/-}$ mice. This model
562 has intact C3a/C3aR and iC3b/CR3 signalling, but lacks C5a/C5b and terminal
563 pathway activity, as do *C3*$^{-/-}$ mice (Figure 5A). We hypothesised that if C*5*$^{-/-}$ mice also
564 displayed enhanced fear-potentiated startle, then the phenotype in *C3*$^{-/-}$ mice would
565 likely be due to a loss of C5a/C5aR signalling or the terminal pathway. On the other
566 hand, if *C5*$^{-/-}$ mice demonstrated normal fear-potentiated startle, this would confine the
567 likely mediating pathway in *C3*$^{-/-}$ mice to iC3b/CR3 signaling (Figure 5A).
568
569 Results from the pre-conditioning session demonstrated increases in the startle
570 response of C*5*$^{-/-}$ mice, (Figure 5B) although in this instance the previously observed
571 enhanced startle reactivity in C*3*$^{-/-}$ mice (Figure 4B) was not replicated. In the
572 conditioning session, there was again evidence of increased startle responses to
573 shock (Figure 5C) in C*3*$^{-/-}$ mice and responses were of a similar magnitude in C*5*$^{-/-}$
574 mice, although these were not significantly different to wildtype. We replicated the
575 previous finding of enhanced fear-potentiated startle in *C3*$^{-/-}$ mice (Figure 5D), but
576 critically both male (Figure 5) and female (Figure S9) *C5*$^{-/-}$ mice showed no evidence
577 of enhanced fear learning and were comparable to wildtypes, indicating that loss of
578 iC3b/CR3 signalling, but not loss of C5a/C5aR and the terminal pathway, was involved
579 in the *C3*$^{-/-}$ fear learning phenotype. Additionally, we did not observe innate anxiety-
580 like phenotypes in *C5*$^{-/-}$ male mice (Figure S5).
581
582 This pattern of effects allowed us to distinguish between the likely mechanisms
583 underlying the enhanced learned fear in *C3*$^{-/-}$ mice, as we could exclude concomitant
584 loss of C5a/C5aR signalling or molecules downstream of C5, and hence also exclude
585 an explanation based on effects of C5a/C5aR signalling on developmental

586 neurogenesis[59,60]. Instead, these data raised the possibility of an explanation based
587 on the established effects of the iC3b/CR3 pathway on synaptic pruning, a mechanism
588 involving microglia mediated elimination of synapses impacting on neurodevelopment
589 and learning-related synaptic plasticity[13,14,61].
590

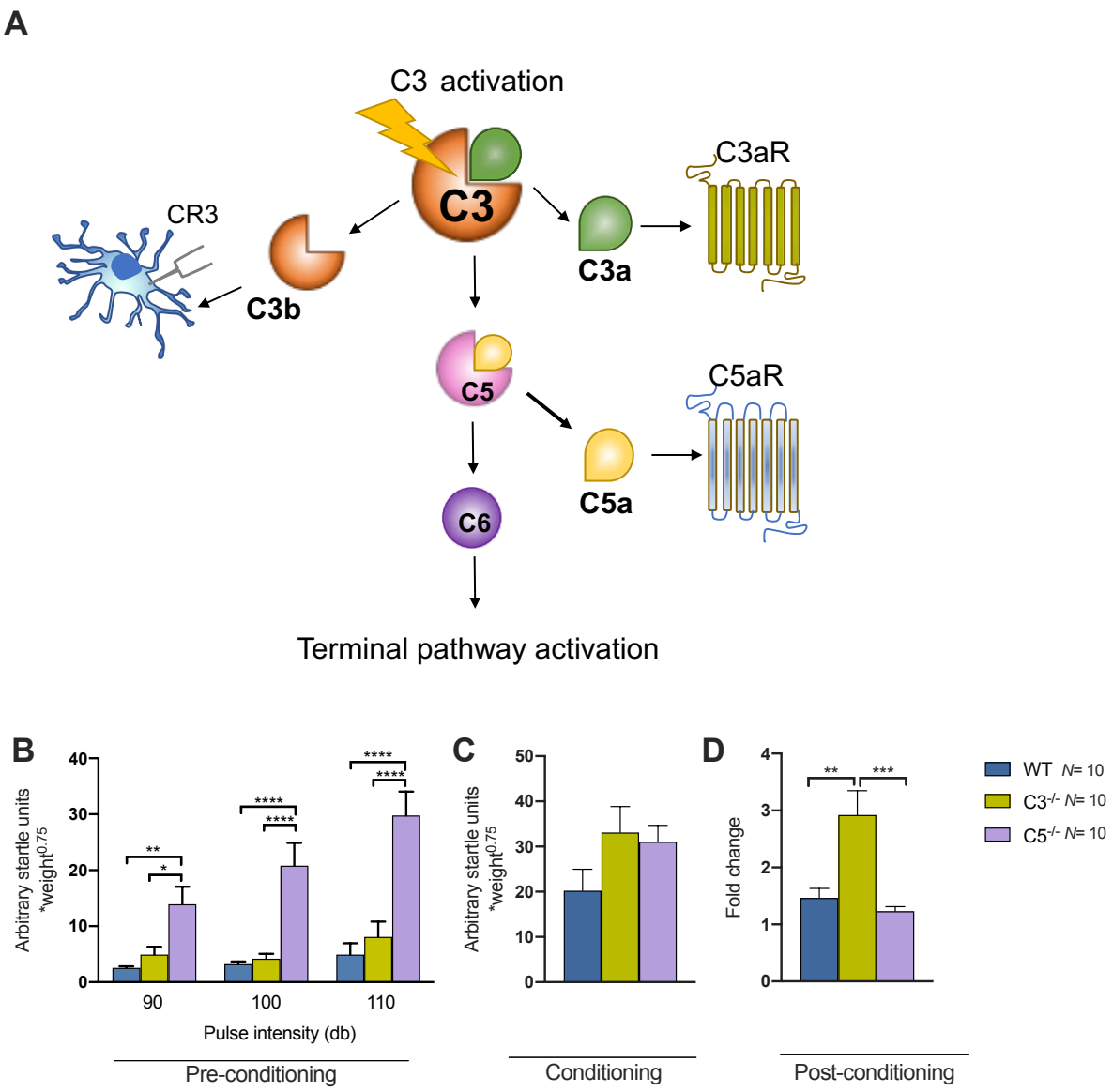

591

592 **Figure 5. Pathways underlying fear learning phenotypes in *C3*$^{-/-}$ mice (A)** C3
593 activation leads to generation of cleavage fragments C3a and C3b. The former signals
594 via C3aR whereas the latter signals via complement receptor 3 (CR3). C3b is also
595 necessary for forming the convertase enzyme that cleaves C5. Upon cleavage, C5

596 generates the fragments C5a and C5b (not shown). C5a signals via the C5aR,
597 whereas C5b propagates activity of the terminal complement pathway via C6. Since
598 C3 cannot be activated in *C3*$^{-/-}$ mice, the action of all these pathways (C3a/C3aR,
599 C3b/CR3, C5a/C5aR, terminal pathway) is absent. By using *C5*$^{-/-}$ mice, which lack
600 C5a/C5aR and terminal pathway activity, we examined whether lack of C3b/CR3,
601 C5a/C5aR or the terminal pathway was responsible for fear learning phenotypes in
602 *C3*$^{-/-}$ mice. **(B)** In the pre-conditioning session there were significant main effects of
603 GENOTYPE ($F_{2,27}$=18.4, p<0.0001) and STIMULUS INTENSITY ($F_{2,54}$=19.0,
604 p<0.0001) and a significant GENOTYPE × STIMULUS INTENSITY interaction
605 ($F_{4,54}$=7.00, p<0.0001). *C5*$^{-/-}$ mice demonstrated increased levels of startle responding
606 relative to wildtype and *C3*$^{-/-}$ mice at all stimulus intensities (90dB; WT 2.55±0.26 vs.
607 *C5*$^{-/-}$ 13.92±3.14, p=0.0069, *C3*$^{-/-}$ 4.92±1.40 vs. *C5*$^{-/-}$ p=0.0405, WT vs. *C3*$^{-/-}$ p=0.7919;
608 100dB; WT 3.23±0.45 vs. *C5*$^{-/-}$ 20.83±4.07, p<0.0001, *C3*$^{-/-}$ 4.924.17±0.88 vs. *C5*$^{-/-}$
609 p<0.0001, WT vs. *C3*$^{-/-}$ p=0.9639; 110dB; WT 4.92±2.03 vs. *C5*$^{-/-}$ 29.78±4.29,
610 p<0.0001, *C3*$^{-/-}$ 8.07±2.76 vs. *C5*$^{-/-}$ p<0.0001, WT vs. *C3*$^{-/-}$ p=0.6643). **(C)** There were
611 no significant differences in startle responses to the footshock+CS pairings during the
612 conditioning session (WT 20.23±4.76, *C3*$^{-/-}$ 33.10±5.74, *C5*$^{-/-}$ 31.08±3.59, $F_{2,27}$=2.10,
613 p=0.1421). **(D)** In the post-conditioning session, all mice demonstrated increases to
614 the pulse+CS stimuli in comparison to pulse-alone stimuli, as demonstrated by the
615 fold-change increase in startle responding, however, this effect was again significantly
616 increased only in *C3*$^{-/-}$ mice (2.92±0.43) relative to wildtype (1.47±0.17, p=0.0020) and
617 *C5*$^{-/-}$ mice (1.23±0.08, p=0.0004, overall ANOVA $F_{2,27}$=11.5, p=0.0002). Data
618 represent mean + S.E.M. *, **, *** and **** represent p≤0.05, p≤0.01, p≤0.001 and
619 p≤0.0001 for *post-hoc* genotype comparisons, respectively.
620

621

622 **3.6 Differential expression of stress and anxiety related genes in *C3aR*$^{-/-}$ and**
623 ***C3*$^{-/-}$ mice**

624 We next sought to assess whether the dissociations in innate anxiety and learned fear
625 between *C3aR*$^{-/-}$ and *C3*$^{-/-}$ models were associated with differential gene expression in
626 brain regions associated with emotional behaviours. We assayed gene expression in
627 male mice, within three regions of recognised importance in stress and anxiety; the
628 medial prefrontal cortex (mPFC), ventral hippocampus (vHPC) and
629 cerebellum[28,62](Figure 6A). Given our previous data showing differential corticosterone
630 responses and altered sensitivity to diazepam in both knockouts, we first measured
631 expression of the glucocorticoid receptor *Nr3c1* and the corticotrophin-releasing
632 hormone receptor 1 *Crhr1*, together with *Gabra2* which encodes the $GABA_A$ receptor
633 α2 subunit responsible for mediating benzodiazepine anxiolysis[63]. There were no
634 effects of genotype on *Crhr1* and *Gabra2* mRNA expression in any of the brain regions
635 assayed (Figure 6B,C). *Nr3c1* expression did however show effects of genotype with
636 trends indicating increases in *C3aR*$^{-/-}$ mice in the mPFC and vHPC, and significantly
637 increased expression in cerebellum that was common to both knockouts (Figure 6D).

638

639 As activation of C3aR has been shown to stimulate calcium influx from the extracellular
640 space[2-4,64,65] and calcium channel subunit variants have strong links to risk for
641 psychiatric and neurological disorders, as well as anxiety phenotypes[66,67], we also
642 investigated a panel of voltage-gated calcium channels. Expression of *Cacna1d,* which
643 encodes the Cav1.3 channel of L-type calcium gated voltage channels, was increased
644 in the mPFC of *C3aR*$^{-/-}$ mice (Figure 6E) and in both *C3*$^{-/-}$ and *C3aR*$^{-/-}$ mice there was
645 upregulation of cerebellar *Cacna1e,* which encodes the Cav2.3 channel of R-type
646 voltage gated calcium channels (Figure 6F). We also investigated the expression of

647 *Cacna1c* which encodes the $Ca_v1.2$ subunit of L-type voltage gated calcium channels
648 that forms the channel pore allowing calcium entry[68]. We found genotype and brain
649 region specific changes in *Cacna1c* expression, with selective increases in expression
650 in *C3aR*$^{-/-}$ mice in the vHPC and cerebellum, but not the mPFC (Figure 6G).
651

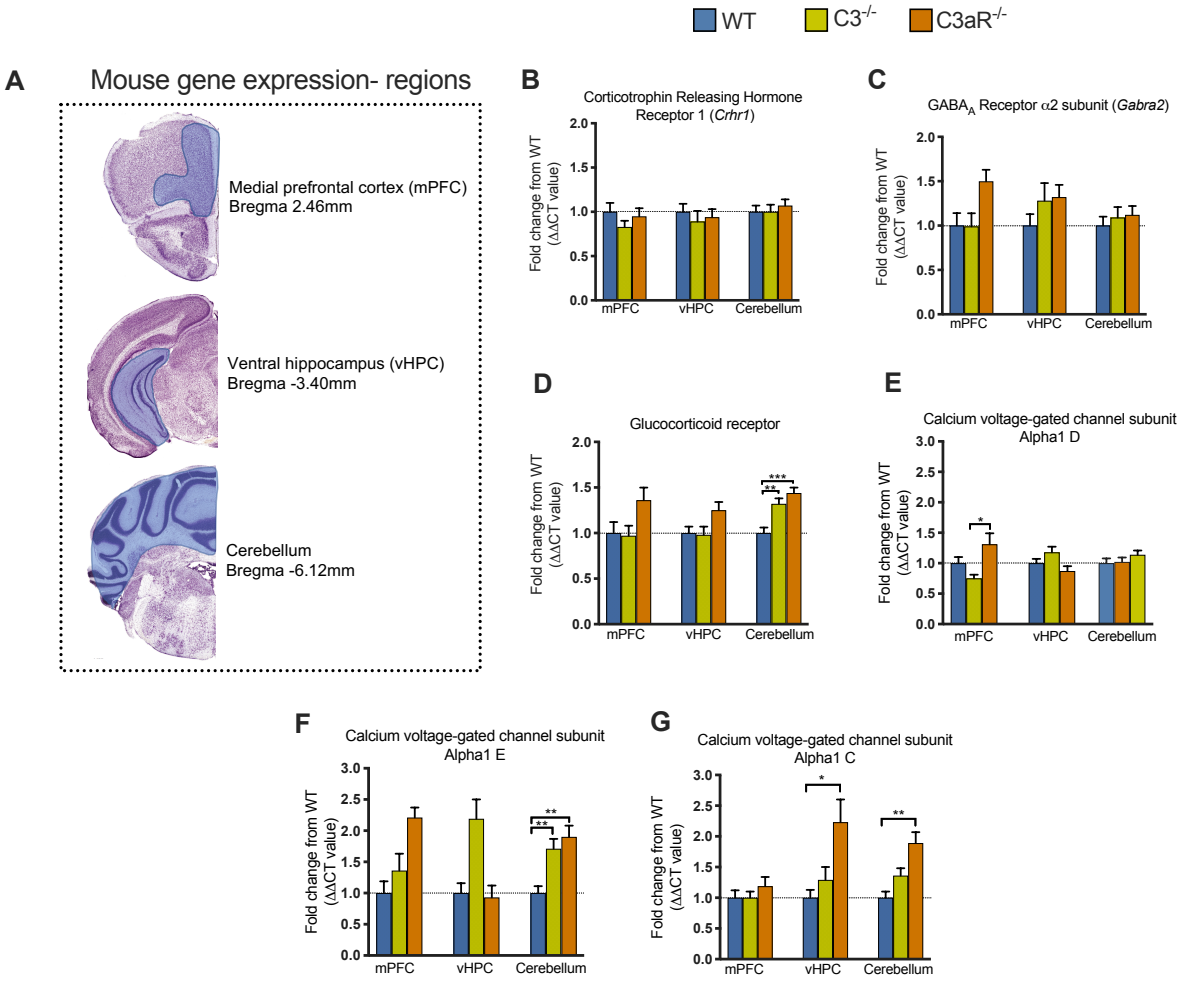

652

653 **Figure 6. mRNA expression of stress and anxiety related genes. (A)** Animals were
654 culled and the medial prefrontal cortex (mPFC), ventral hippocampus (vHPC) and
655 cerebellum were dissected. **(B)** There were no significant differences in the expression
656 of Corticotrophin releasing hormone receptor 1 (*Crhr1*) in any region, across
657 genotypes (mPFC $F_{2,53}$=0.587, p=0.5597, N wildtype=20, *C3*$^{-/-}$=17, *C3aR*$^{-/-}$= 19; vHPC
658 $F_{2,49}$=0.169, p=0.8450, N WT=20, *C3*$^{-/-}$=15, *C3aR*$^{-/-}$= 17; cerebellum $F_{2,47}$=0.0482,

659 p=0.8346, N WT=19, *C3*$^{-/-}$=17, *C3aR*$^{-/-}$= 14). **(C)** There were also no significant
660 changes in the expression of the $GABA_A$ receptor α2 subunit (*Gabra2*) in any region,
661 across genotypes (mPFC H_2=1.04, p=0.5939, N wildtype=20, *C3*$^{-/-}$=19, *C3aR*$^{-/-}$= 16;
662 vHPC $F_{2,49}$=0.721, p=0.4914, N WT=20, *C3*$^{-/-}$=13, *C3aR*$^{-/-}$= 19; cerebellum
663 $F_{2,47}$=0.221, p=0.8026, N WT=18, *C3*$^{-/-}$=17, *C3aR*$^{-/-}$= 15). **(D)** Expression of the
664 glucocorticoid receptor (*Nr3c1*) was significantly increased in the cerebellum of both
665 *C3*$^{-/-}$ and *C3aR*$^{-/-}$ groups ($F_{2,61}$=10.3, p=0.0002, *C3*$^{-/-}$ vs. wildtype p=0.0023, *C3aR*$^{-/-}$ vs.
666 wildtype p=0.0002, N wildtype=19, *C3*$^{-/-}$=20, *C3aR*$^{-/-}$= 15). There were trends towards
667 increased expression of the glucocorticoid receptor gene *Nr3c1* in the mPFC and
668 vHPC of *C3aR*$^{-/-}$ mice but these were not significant (mPFC; $F_{2,56}$=1.33, p=0.2723, N
669 wildtype=20, *C3*$^{-/-}$=20, *C3aR*$^{-/-}$= 19, vHPC; $F_{2,62}$=1.11, p=0.3345, N wildtype=23, *C3*$^{-/-}$
670 =20, *C3aR*$^{-/-}$= 22). **(E)** Calcium voltage-gated channel subunit Alpha 1d (*Cacna1d*)
671 expression was changed in the mPFC ($F_{2,36}$=7.52, p=0.0407) owing to altered
672 expression between *C3*$^{-/-}$ and *C3aR*$^{-/-}$ mice (p=0.0314; N wildtype=11, *C3*$^{-/-}$=13, *C3aR*$^{-}$
673 $^{/-}$= 15). There were no differences in the vHPC ($F_{2,31}$=2.27, p=0.1199, N wildtype=14,
674 *C3*$^{-/-}$=10, *C3aR*$^{-/-}$= 10) or cerebellum ($F_{1,39}$=0.648, p=0.5286, N wildtype=14, *C3*$^{-/-}$=16,
675 *C3aR*$^{-/-}$= 12). **(F)** Expression of the Calcium voltage-gated channel subunit Alpha 1e
676 (*Cacna1e*) was significantly upregulated in the cerebellum of both knockouts
677 ($F_{2,39}$=7.52, p=0.0017, wildtype vs. *C3*$^{-/-}$ p=0.0082, wildtype vs. *C3aR*$^{-/-}$ p=0.0032; N
678 wildtype=14, *C3*$^{-/-}$=16, *C3aR*$^{-/-}$= 12). There were borderline significant changes in
679 expression in the vHPC ($F_{2,32}$=3.15, p=0.0565, N wildtype=14, *C3*$^{-/-}$=11, *C3aR*$^{-/-}$= 10)
680 and no significant changes in the mPFC (H_2=3.43, p=0.1802, N wildtype=11, *C3*$^{-/-}$=12,
681 *C3aR*$^{-/-}$= 15).**(G)** Expression levels of the Calcium voltage-gated channel subunit
682 Alpha 1c (*Cacna1c*) were significantly increased in *C3aR*$^{-/-}$ mice in a regionally specific
683 manner in the vHPC ($F_{2,47}$=3.20, p=0.0496, *C3*$^{-/-}$ vs. wildtype p=0.6895, *C3aR*$^{-/-}$ vs.

684 wildtype p=0.0295, N wildtype=21, *C3*$^{-/-}$=13, *C3aR*$^{-/-}$= 16) and the cerebellum
685 ($F_{2,54}$=5.84, p=0.0051, *C3*$^{-/-}$ vs. wildtype p=0.1613, *C3aR*$^{-/-}$ vs. wildtype p=0.0024, N
686 wildtype=20, *C3*$^{-/-}$=20, *C3aR*$^{-/-}$= 17). There were no significant changes in the mPFC
687 ($F_{2,52}$=1.04, p=0.5939, N wildtype=20, *C3*$^{-/-}$=19, *C3aR*$^{-/-}$= 16). Data represent fold
688 change from wildtype + SEM. *, **, *** represent p≤0.05, p≤0.01 and p≤0.001 for *post-*
689 *hoc* genotype comparisons, respectively.
690
691
692 **4. Discussion**
693 We have used knockout models manipulating specific complement proteins to reveal
694 dissociable effects of complement pathways on distinct elements of aversive
695 behaviours. A main finding was a profound innate anxiety phenotype in the *C3aR*$^{-/-}$
696 mice that was absent in *C3*$^{-/-}$ mice. The specificity of the anxiety phenotype exhibited
697 by *C3aR*$^{-/-}$ mice at the behavioural level was paralleled by EPM-evoked corticosterone
698 levels, confirming the validity of the EPM as an index of anxiety-like behaviour. A
699 second main finding was a double dissociation in terms of fear learning, whereby *C3*$^{-}$
700 $^{/-}$ and not *C3aR*$^{-/-}$ mice displayed enhanced conditioned fear reactivity. Using *C5*$^{-/-}$
701 mice, we conclude that the mechanisms accounting for the fear learning phenotype in
702 *C3*$^{-/-}$ mice are likely to arise from lack of iC3b/CR3 pathway activity. These data
703 indicate distinct effects mediated by closely related elements of the complement
704 system that differentially impact upon the neural mechanisms underlying innate
705 anxiety and learned fear.
706
707 Our findings extend previous findings of abnormal anxiety behaviour in *C3aR*$^{-/-}$ mice[35]
708 . Our use of specific complement knockout models allowed us to further pinpoint the

709 likely complement pathways and potential mechanisms underlying C3aR-mediated
710 anxiety. Since C3a is solely produced via C3 cleavage, and C3aR is the canonical
711 receptor for C3a, we expected that any phenotypes dependent on the binding of C3a
712 to the C3aR would be apparent in both *C3*$^{-/-}$ and *C3aR*$^{-/-}$ models. However, this was
713 not borne out in our data. Given the divergence in phenotypes seen, one explanation
714 is that the *C3aR*$^{-/-}$ anxiety phenotypes are independent of C3a and instead mediated
715 by an alternative ligand. It has long been speculated that there may be promiscuity of
716 the C3aR due to its unusually large second extracellular loop[69]. Indeed, a cleavage
717 fragment of the neuropeptide precursor protein VGF (non-acronymic), TLQP-21, was
718 recently reported to bind the C3aR[70,71]. This peptide has pleiotropic roles including in
719 the stress response[72] and its precursor VGF is widely expressed throughout the CNS[73]
720 and in regions associated with stress reactivity such as the hypothalamus, where there
721 is evidence for C3aR expression[74,75]. Determining whether the mechanisms
722 underlying innate anxiety phenotypes in *C3aR*$^{-/-}$ mice are dependent on TLQP-
723 21/C3aR interactions will be a priority for future work.
724
725 Whether the *C3aR*$^{-/-}$ phenotypes described here are the result of ongoing effects of
726 *C3aR* deletion in the adult brain or instead the enduring consequence of
727 neurodevelopmental impacts of *C3aR* deficiency also remains to be determined. On
728 the basis of previous findings implicating C3aR in both developmental neurogenesis[76]
729 and in acute brain changes following behavioural manipulations[77], both are
730 possibilities. One strategy would be to test whether acute administration of the C3aR
731 antagonist SB290157[78] phenocopies the constitutive knockout of *C3aR*, though at
732 present no data is available on the CNS penetration of SB290157 and this molecule
733 has received criticism due to evidence of agonist activity[79].

734

735 We also probed mechanisms underpinning the *C3aR*$^{-/-}$ innate anxiety phenotype by
736 assessing the effects of the anxiolytic drug diazepam. We found that a dose of
737 diazepam that was anxiolytic in wildtype mice had no effect in *C3aR*$^{-/-}$ mice. Stretch
738 attend postures, thought to reflect risk assessment behaviour[54], are highly sensitive to
739 pharmacological manipulation[50,80] and in agreement with our own findings, diazepam
740 has been shown to specifically decrease SAPs in the absence of effects on open arm
741 exploration[81]. Importantly, *C3aR*$^{-/-}$ mice consistently performed more SAPs than other
742 genotypes, and therefore floor effects cannot account for the pattern of results
743 observed. Benzodiazepines act on $GABA_A$ receptors[63] however we found no
744 significant changes in expression of *Gabra2*, a $GABA_A$ receptor subunit responsible
745 for anxiolytic actions of benzodiazepines in tests of innate anxiety[63], in the brain
746 regions sampled. This raises the possibility of alternative molecular mechanisms
747 mediating the anxiety phenotypes seen in the *C3aR*$^{-/-}$ model. Whatever the molecular
748 underpinnings of the dissociable anxiety phenotypes, our data show a profoundly
749 altered effect of diazepam in both knockouts; a lack of response in *C3aR*$^{-/-}$ and an
750 apparent paradoxical anxiogenic effect of the drug in *C3*$^{-/-}$ mice, though this
751 interpretation needs to take into account an apparent selective sedative effect in *C3*$^{-/-}$
752 mice.

753

754 In contrast to innate anxiety, we observed a specific effect of *C3* knockout on
755 conditioned fear. The absence of a comparable phenotype in *C3aR*$^{-/-}$ and *C5*$^{-/-}$ mice
756 suggested that these effects were unlikely to be due to loss of either C3a/C3aR,
757 C5a/C5aR, or the terminal pathway, and instead that enhanced fear learning
758 phenotypes in *C3*$^{-/-}$ mice were likely dependent on loss of the iC3b/CR3 pathway. This

759 pathway has been strongly implicated in activity dependent synaptic elimination during
760 neurodevelopment[13,25] and in age-dependent synapse loss[82]. While demonstrations
761 of complement mediated synaptic pruning during development have centered on the
762 visual system, complement-mediated microglial phagocytosis of dopamine D1
763 receptors has been demonstrated in the nucleus accumbens with functional impacts
764 on social behaviour[83]. It remains to be seen whether complement mediated processes
765 of this nature, within brain regions linked to fear processing such as the ventral
766 hippocampus, amygdala and prefrontal cortex are responsible for enhanced fear
767 learning in *C3*$^{-/-}$ mice, or whether this phenotype is a general consequence of altered
768 synaptic elimination throughout the *C3*$^{-/-}$ brain. In addition to developmental processes,
769 the iC3b/CR3 pathway could also be involved acutely in fear learning. *C3* mRNA is
770 upregulated during discrete stages of fear learning[77] and microglial CR3 is implicated
771 in long term depression[84]. Furthermore, complement-mediated engulfment of
772 synapses by microglia may be important in the forgetting of fear memories[14].
773
774 At the gene expression level, we found some changes which were common to both
775 knockouts, and one result that was specific to *C3aR*$^{-/-}$ mice. Regarding the latter, there
776 was a highly specific increase in expression of *Cacna1c* in the ventral hippocampus
777 and cerebellum of *C3aR*$^{-/-}$ mice. This finding is of potential interest given the strong
778 evidence implicating *CACNA1C* variants in genetic risk for a broad spectrum of
779 psychiatric disorders including schizophrenia and bipolar disorder[66], with anxiety
780 phenotypes reported in both human risk variant carriers[85] and animal models[86-89].
781 Furthermore, recent evidence indicates convergent polygenic mechanisms shared
782 between complement and other psychiatric risk genes[90], including calcium regulation
783 pathways, and thus our study lends further support to an interaction between these

784 systems. Whether alterations in *Cacna1c* are of direct functional relevance to the
785 *C3aR*$^{-/-}$ anxiety phenotypes observed here remains to be determined experimentally.
786 We also observed increased cerebellar expression of the glucocorticoid receptor in
787 both *C3*$^{-/-}$ and *C3aR*$^{-/-}$ mice, suggesting that these alterations may result from the
788 absence of C3a/C3aR signalling. Expression of these genes did not differentiate
789 between models and therefore were unlikely to contribute to the dissociable effects of
790 the knockouts on behaviour and stress hormone physiology. Future studies of
791 neuronal activity in brain regions linked to emotion may be more informative in terms
792 of functional neuroanatomy underlying the anxiety-related behavioural and
793 physiological differences seen in the knockout models.
794
795 Anxiety and fear are commonly comorbid with depression and recent preclinical work
796 has suggested a protective role for C3a/C3aR in chronic-stress induced depressive-
797 behaviour[91]. Given the common co-occurrence of anxiety and depression, our findings
798 of enhanced anxiety in *C3aR*$^{-/-}$ mice might seem at odds with the reported resilience
799 of this strain^{-} to depression-related phenotypes[91]. However, the chronic unpredictable-
800 stress paradigm used in these studies is likely to evoke significant inflammation, and
801 therefore the extent to which our data in acutely stressed animals can be compared is
802 questionable. In summary, our findings add significantly to the evidence that
803 perturbations of the complement system, whether reduced complement activation as
804 in the present work or excessive activation as is predicted by *C4* genetic variants[24,92],
805 have major and dissociable effects on brain and behavioural phenotypes of relevance
806 to core clinical symptoms of psychiatric disease.
807
808

809 **5. Author's contributions**

810 The study was designed by LJW, TH, BPM, WPG and LSW. LJW and TH performed
811 behavioural experiments with assistance from NH. Molecular analyses were
812 performed by SAB, EB, MT, ALM, AIB and LJW. Data interpretation were carried out
813 by JH, MJO, JR, WPG, NH, TRH, BPM, LSW and TH. The manuscript was drafted by
814 LJW, TH, WPG and LSW. All authors approved the final manuscript.

815

816 **6. Acknowledgements**

817 The authors thank Professor Craig Gerard and Professor Marina Botto for provision of
818 the *C3aR*$^{-/-}$ and *C5*$^{-/-}$ strains respectively, and to Rhys Perry, Pat Mason, Helen Read
819 and other staff at Cardiff University BIOSV for their invaluable animal care and
820 husbandry. This work was supported by a Wellcome Trust Integrative Neuroscience
821 PhD Studentship awarded to LJW (099816/Z/12/Z), a Waterloo Foundation Early
822 Career Fellowship awarded to LJW, a Hodge Centre for Neuropsychiatric Immunology
823 Seed Corn and Project grant awarded to LJW and a Wellcome Trust Strategic Award
824 100202/Z/12/Z (DEFINE) held by the Neuroscience and Mental Health Research
825 Institute at Cardiff University.

826

827 **7. Competing financial interests**

828 The authors declare no competing financial interests.

829

830 **8. Materials and correspondence**

831 All data from this study are available from the corresponding authors upon reasonable
832 request.

833

9. References

1. Coulthard, L. G. & Woodruff, T. M. Is the Complement Activation Product C3a a Proinflammatory Molecule? Re-evaluating the Evidence and the Myth. *J. Immunol.* **194,** 3542–3548 (2015).
2. Norgauer, J. *et al.* Complement fragment C3a stimulates Ca2+ influx in neutrophils via a pertussis-toxin-sensitive G protein. *Eur. J. Biochem.* **217,** 289–294 (1993).
3. Möller, T., Nolte, C., Burger, R., Verkhratsky, A. & Kettenmann, H. Mechanisms of C5a and C3a Complement Fragment-Induced [Ca2+]i Signaling in Mouse Microglia. *Journal of Neuroscience* **17,** 615–624 (1997).
4. Lian, H., Li, Y., Lu, H.-C. & Zheng, H. NFκB-Activated Astroglial Release of Complement C3 Compromises Neuronal Morphology and Function Associated with Alzheimer's Disease. **85,** 101–115 (2015).
5. Sayah, S. *et al.* Two different transduction pathways are activated by C3a and C5a anaphylatoxins on astrocytes. *Molecular Brain Research* **112,** 53–60 (2003).
6. Morley, B. J. & Walport, M. J. *The Complement FactsBook*. (Academic Press, 1999).
7. Kemper, C. & Köhl, J. Back to the future – non-canonical functions of complement. *Seminars in Immunology* **37,** 1–3 (2018).
8. Nataf, S., Stahel, P. F., Davoust, N. & Barnum, S. R. Complement anaphylatoxin receptors on neurons: new tricks for old receptors? *Trends Neurosci.* **22,** 397–402 (1999).
9. Veerhuis, R., Nielsen, H. M. & Tenner, A. J. Complement in the brain. *Molecular Immunology* **48,** 1592–1603 (2011).
10. Bénard, M., Gonzalez, B. J., Biological, M. S. J. O.2004. Characterization of C3a and C5a receptors in rat cerebellar granule neurons during maturation neuroprotective effect of C5a against apoptotic cell death. *J Biol. Chem,* **42***,* 43487-43496 (2004).
11. Rahpeymai, Y. *et al.* Complement: a novel factor in basal and ischemia-induced neurogenesis. *EMBO J* **25,** 1364–1374 (2006).
12. Gorelik, A. *et al.* Developmental activities of the complement pathway in migrating neurons. *Nature Communications* **8,** 15096 (2017).
13. Stevens, B. *et al.* The classical complement cascade mediates CNS synapse elimination. *Cell* **131,** 1164–1178 (2007).
14. Wang, C. *et al.* Microglia mediate forgetting via complement-dependent synaptic elimination. *Science,* **367,** 688-694 (2020).
15. Harold, D. *et al.* Genome-wide association study identifies variants at CLU and PICALM associated with Alzheimer's disease. *Nature Genetics* **41,** 1088–1093 (2009).
16. Jansen, I. E. *et al.* Genome-wide meta-analysis identifies new loci and functional pathways influencing Alzheimer's disease risk. *Nature Genetics* **51**, 404–413 (2019).
17. Shi, Q. *et al.* Complement C3-Deficient Mice Fail to Display Age-Related Hippocampal Decline. *Journal of Neuroscience* **35,** 13029–13042 (2015).
18. Zhou, J., Fonseca, M. I., Pisalyaput, K. & Tenner, A. J. Complement C3 and C4 expression in C1q sufficient and deficient mouse models of Alzheimer’s disease. *Journal of Neurochemistry* **106,** 2080–2092 (2008).

19. Corbett, B. A. *et al.* A proteomic study of serum from children with autism showing differential expression of apolipoproteins and complement proteins. *Mol. Psychiatry* **12,** 292 (2007).
20. Maes, M., Delange, J., Ranjan, R., Meltzer, H. Y. & Desnyer, R. Acute phase proteins in schizophrenia, mania and major depression: modulation by psychotropic drugs. *Pharmacology Biochemistry and Behaviour* 1–11 (1997). doi:10.1016/S0165-1781(96)02915-0
21. Ruland, T. *et al.* Molecular serum signature of treatment resistant depression. *Psychopharmacology* 1–9 (2016).
22. Song, Y. R. *et al.* Specific alterations in plasma proteins during depressed, manic, and euthymic states of bipolar disorder. *Brazilian Journal of Medical and Biological Research* **48,** 973–982
23. Oganesyan, L. P., Mkrtchyan, G. M., Sukiasyan, S. H. & Boyajyan, A. S. Classic and alternative complement cascades in post-traumatic stress disorder. *Bull. Exp. Biol. Med.* **148,** 859–861 (2009).
24. Sekar, A. *et al.* Schizophrenia risk from complex variation of complement component 4. *Nature,* ***530,*** 117–183 (2016).
25. Schafer, D. P. *et al.* Microglia Sculpt Postnatal Neural Circuits in an Activity and Complement-Dependent Manner. *Neuron* **74,** 691–705 (2012).
26. Håvik, B. *et al.* The Complement Control-Related Genes CSMD1 and CSMD2 Associate to Schizophrenia. *BPS* **70,** 35–42 (2011).
27. Zhang, S. *et al.* Association Between Polymorphisms of the Complement 3 Gene and Schizophrenia in a Han Chinese Population. *Cell. Physiol. Biochem.* **46,** 2480–2486 (2018).
28. Tovote, P., Fadok, J. P. & Lüthi, A. Neuronal circuits for fear and anxiety. *Nat. Rev.* **16,** 317–331 (2015).
29. Perusini, J. N. & Fanselow, M. S. Neurobehavioral perspectives on the distinction between fear and anxiety. *Learn. Mem.* **22,** 417–425 (2015).
30. Davis, M. Neural systems involved in fear and anxiety measured with fear-potentiated startle. *Am Psychol* **61,** 741–756 (2006).
31. Engin, E. *et al.* Modulation of anxiety and fear via distinct intrahippocampal circuits. . *eLife,* **5:e14120**, (2016).
32. Yilmaz, M. *et al.* Overexpression of schizophrenia susceptibility factor human complement C4A promotes excessive synaptic loss and behavioral changes in mice. *Nat Neurosci* 1–31 (2020).
33. Girardi, G. *et al.* Imaging of activated complement using ultrasmall superparamagnetic iron oxide particles (USPIO)-conjugated vectors: An in vivo in utero non-invasive method to predict placental insufficiency and abnormal fetal brain development. *Mol. Psychiatry* **20,** 1017–1026 (2015).
34. Kulkarni, A. P., Govender, D. A., Kotwal, G. J. & Kellaway, L. A. Modulation of anxiety behavior by intranasally administered Vaccinia virus complement control protein and curcumin in a mouse model of Alzheimer's disease. *Current Alzheimer Research* **8,** 95–113 (2011).
35. Pozo-Rodrigálvarez, A., Ollaranta, R., Skoog, J., Pekny, M. & Pekna, M. Hyperactive Behavior and Altered Brain Morphology in Adult Complement C3a Receptor Deficient Mice. *Front. Immunol.* **12,** 604812 (2021).
36. Fischer, M. B., Ma, M., Goerg, S., Zhou, X. & Xia, J. Regulation of the B cell response to T-dependent antigens by classical pathway complement. *J.Immunol,* **157,** 549-556, (1996).

37. Humbles, A. A. *et al*. A role for the C3a anaphylatoxin receptor in the effector phase of asthma. *Nature,* **406,** 998–1001 (2000).
38. Wang, Y. *et al.* A role for complement in antibody-mediated inflammation: C5-deficient DBA/1 mice are resistant to collagen-induced arthritis. *J. Immunol.* **164,** 4340–4347 (2000).
39. Mikaelsson, M. A., ncia, M. C. A., Dent, C. L., Wilkinson, L. S. & Humby, T. Placental programming of anxiety in adulthood revealed by Igf2-null models. *Nature Communications* **4,** 1–9 (2013).
40. Molewijk, H. E., van der Poel, A. M. & Olivier, B. The ambivalent behaviour 'stretched approach posture' in the rat as a paradigm to characterize anxiolytic drugs. *Psychopharmacology* **121,** 81–90
41. Mackintosh, J. H. & Grant, E. C. A Comparison of the Social Postures of Some Common Laboratory Rodents. *Behaviour* **21,** 246–259 (1963).
42. Kleiber, M. Body size and metabolism. *Hilgardia Journal of Agricultural Science* **6,** 315–353 (1932).
43. Mikaelsson, M. A., Constância, M., Dent, C. L., Wilkinson, L. S. & Humby, T. Placental programming of anxiety in adulthood revealed by Igf2-null models. *Nature Communications* **4,** 2311 (2013).
44. Dickmeis, T. Glucocorticoids and the circadian clock. *Journal of Endocrinology* **200,** 3–22 (2008).
45. Livak, K. J. & Schmittgen, T. D. Analysis of Relative Gene Expression Data Using Real-Time Quantitative PCR and the 2−ΔΔCT Method. *Methods* **25,** 402–408 (2001).
46. Wright, S. P. Adjusted p-values for simultaneous inference. *Biometrics* **48,** 1005–1013 (1992).
47. Pellow, S., Chopin, P., File, S. E. & Briley, M. Validation of open : closed arm entries in an elevated plus-maze as a measure of anxiety in the rat. *J. Neurosci. Methods* **14,** 149–167 (1985).
48. Walf, A. A. & Frye, C. A. The use of the elevated plus maze as an assay of anxiety-related behavior in rodents. *Nat Protoc* **2,** 322–328 (2007).
49. Ennaceur, A. Tests of unconditioned anxiety - pitfalls and disappointments. *Physiology & Behavior* **135,** 55–71 (2014).
50. RODGERS, R. J. Anxiety, defence and the elevated plus-maze. *Pharmacology Biochemistry and Behaviour* (1997).
51. Braun, A. A., Skelton, M. R., Vorhees, C. V. & Williams, M. T. Comparison of the elevated plus and elevated zero mazes in treated and untreated male Sprague-Dawley rats: Effects of anxiolytic and anxiogenic agents. *Pharmacology Biochemistry and Behavior* **97,** 406–415 (2011).
52. Lepicard, E. M., Joubert, C., Hagneau, I., Perez-Diaz, F. & Chapouthier, G. Differences in anxiety-related behavior and response to diazepam in BALB/cByJ and C57BL/6J strains of mice. *Pharmacology Biochemistry and Behavior* **67,** 739–748 (2000).
53. Grewal, S. S., Sherperd, D, J. K., Bill, D. J., Fletcher, A. & Dourish, C. T. Behavioural and pharmacological characterisation of the canopy stretched attend posture test as a model of anxiety in mice and rats. *Psychopharmacology* **133,** 29–38 (1997).
54. Kaesermann, H. P. Stretched attend posture, a non-social form of ambivalence, is sensitive to a conflict-reducing drug action. *Psychopharmacology* **89,** 31–37

55. Albrechet-Souza, L., Cristina de Carvalho, M., Rodrigues Franci, C. & Brandão, M. L. Increases in plasma corticosterone and stretched-attend postures in rats naive and previously exposed to the elevated plus-maze are sensitive to the anxiolytic-like effects of midazolam. *Hormones and Behavior* **52,** 267–273 (2007).
56. Holt, D. J., Coombs, G., Zeidan, M. A., Goff, D. C. & Milad, M. R. Failure of neural responses to safety cues in schizophrenia. *Arch Gen Psychiatry* **69,** 893–903 (2012).
57. Grillon, C., Morgan, C. A., Southwick, S. M., Davis, M. & Charney, D. S. Baseline startle amplitude and prepulse inhibition in Vietnam veterans with posttraumatic stress disorder. *Psychiatry Research* **64,** 169–178 (1996).
58. Falls, W. A., Carlson, S., Turner, J. G. & Willott, J. F. Fear-potentiated startle in two strains of inbred mice. *Behavioral Neuroscience* **111,** 855–861 (1997).
59. Coulthard, L. G. *et al.* Complement C5aR1 Signaling Promotes Polarization and Proliferation of Embryonic Neural Progenitor Cells through PKCζ. *J. Neurosci.* **37,** 5395–5407 (2017).
60. Hawksworth, O. A., Coulthard, L. G., Taylor, S. M., Wolvetang, E. J. & Woodruff, T. M. Brief Report: Complement C5a Promotes Human Embryonic Stem Cell Pluripotency in the Absence of FGF2. *Stem Cells,* **32,** 3278-3284, (2014).
61. Schafer, D. P. *et al.* Microglia sculpt postnatal neural circuits in an activity and complement-dependent manner. *Neuron* **74,** 691–705 (2012).
62. Apps, R. & Strata, P. Neuronal circuits for fear and anxiety - the missing link. *Nat. Rev.* **16,** 642 (2015).
63. Smith, K. S., Engin, E., Meloni, E. G. & Rudolph, U. Benzodiazepine-induced anxiolysis and reduction of conditioned fear are mediated by distinct GABAA receptor subtypes in mice. *Neuropharmacology* **63,** 250–258 (2012).
64. Ahamed, J., Venkatesha, R. T., Thangam, E. B. & Ali, H. C3a Enhances Nerve Growth Factor-Induced NFAT Activation and Chemokine Production in a Human Mast Cell Line, HMC-1. *J. Immunol.* **172,** 6961–6968 (2004).
65. Wu, F. *et al.* Complement component C3a plays a critical role in endothelial activation and leukocyte recruitment into the brain. *J Neuroinflammation* **13,** 23 (2016).
66. Hamshere, M. L. *et al.* Genome-wide significant associations in schizophrenia to ITIH3/4, CACNA1C and SDCCAG8, and extensive replication of associations reported by the Schizophrenia PGC. *Mol. Psychiatry* 1–5 (2019).
67. Kabir, Z. D. *et al.* Rescue of impaired sociability and anxiety-like behavior in adult cacna1c-deficient mice by pharmacologically targeting eIF2α. *Mol. Psychiatry* **22,** 1096–1109 (2017).
68. Simms, B. A. & Zamponi, G. W. Neuronal Voltage-Gated Calcium Channels: Structure, Function, and Dysfunction. *Neuron* **82,** 24–45 (2014).
69. Chao, T. H. *et al.* Role of the second extracellular loop of human C3a receptor in agonist binding and receptor function. *Journal of Biological Chemistry* **274,** 9721–9728 (1999).

70. Hannedouche, S. *et al.* Identification of the C3a Receptor (C3AR1) as the Target of the VGF-derived Peptide TLQP-21 in Rodent Cells. *Journal of Biological Chemistry* **288,** 27434–27443 (2013).
71. Cero, C. *et al.* The TLQP-21 peptide activates the G-protein-coupled receptor C3aR1 via a folding-upon-binding mechanism. *Structure* **22,** 1744–1753 (2014).
72. Razzoli, M. *et al.* Implication of the VGF-derived peptide TLQP-21 in mouse acute and chronic stress responses. *Behav. Brain Res.* **229,** 333–339 (2012).
73. van den Pol, A. N., Bina, K., Decavel, C. & Ghosh, P. VGF expression in the brain. *J. Comp. Neurol.* **347,** 455–469 (1994).
74. Lewis, B., Francis, K., Gasque, P., Scanlon, M. & Ham, J. Functional complement C3a receptors in the rat pituitary gland. *Endocrine Abstracts* **3,** 198 (2002).
75. Francis, K. Complement C3a receptors in the pituitary gland: a novel pathway by which an innate immune molecule releases hormones involved in the control of inflammation. *The FASEB Journal* 1–4 (2003).
76. Coulthard, L. G., Hawksworth, O. A. & Woodruff, T. M. Complement: The Emerging Architect of the Developing Brain. *Trends Neurosci.* **41,** 373–384 (2018).
77. Scholz, B. *et al.* The Regulation of Cytokine Networks in Hippocampal CA1 Differentiates Extinction from Those Required for the Maintenance of Contextual Fear Memory after Recall. *PLoS ONE* **11,** e0153102–29 (2016).
78. Ames, R. S. *et al.* Identification of a selective nonpeptide antagonist of the anaphylatoxin C3a receptor that demonstrates anti-inflammatory activity in animal models. *J. Immunol.* **166,** 6341–6348 (2001).
79. Therien, A. G., Baelder, R. & Köhl, J. Agonist Activity of the Small Molecule C3aR Ligand SB 290157. *J. Immunol.* **174,** 7479–7480 (2005).
80. Holly, K. S., Orndorff, C. O. & Murray, T. A. MATSAP: An automated analysis of stretch-attend posture in rodent behavioral experiments. *Scientific Reports* **6,** (2016).
81. Genewsky, A. *et al.* How much fear is in anxiety? BioRxiv preprint doi:10.1101/385823
82. Hong, S. *et al.* Complement and microglia mediate early synapse loss in Alzheimer mouse models. *Science* **352,** 712–716 (2016).
83. Kopec, A. M., Smith, C. J., Ayre, N. R., Sweat, S. C. & Bilbo, S. D. Microglial dopamine receptor elimination defines sex-specific nucleus accumbens development and social behavior in adolescent rats. *Nature Communications* **9,** 3769 (2018).
84. Zhang, J. *et al.* Microglial CR3 Activation Triggers Long-Term Synaptic Depression in the Hippocampus via NADPH Oxidase. *Neuron* **82,** 195–207 (2014).
85. Roussos, P., Giakoumaki, S. G., Georgakopoulos, A., Robakis, N. K. & Bitsios, P. The CACNA1C and ANK3 risk alleles impact on affective personality traits and startle reactivity but not on cognition or gating in healthy males. *Bipolar Disorders* **13,** 250–259 (2011).
86. Bader, P. L. *et al.* Mouse model of Timothy syndrome recapitulates triad of autistic traits. *Proc. Natl. Acad. Sci. U.S.A.* **108,** 15432–15437 (2011).

87. Lee, A. S. *et al.* Forebrain elimination of cacna1c mediates anxiety-like behavior in mice. *Nat.Neurosci* **17,** 1054–1055 (2012).
88. Dao, D. T. *et al.* Mood Disorder Susceptibility Gene CACNA1C Modifies Mood-Related Behaviors in Mice and Interacts with Sex to Influence Behavior in Mice and Diagnosis in Humans. *Biological Psychiatry* **68,** 801–810 (2010).
89. Dedic, N. *et al.* Cross-disorder risk gene CACNA1C differentially modulates susceptibility to psychiatric disorders during development and adulthood. *Nat.Neurosci* **23,** 533–543 (2018).
90. Kim, M. *et al.* Brain gene co-expression networks link complement signaling with convergent synaptic pathology in schizophrenia. *Nat Neurosci* **24,** 799–809 (2021).
91. Crider, A. *et al.* Complement component 3a receptor deficiency attenuates chronic stress-induced monocyte infiltration and depressive-like behavior. *Brain, Behavior, and Immunity* **70,** 246–256 (2018).
92. Sellgren, C. M. *et al.* Increased synapse elimination by microglia in schizophrenia patient-derived models of synaptic pruning. *Nat.Neurosci* **22,** 1–385 (2019).